PROCEEDINGS OF SPIE

Nanostructured Thin Films II

Geoffrey B. Smith
Akhlesh Lakhtakia
Cheng-Chung Lee
Editors

5–6 August 2009
San Diego, California, United States

Volume 7404

SPIE

Please use the following format to cite material from this book:
Author(s), "Title of Paper," in *Nanostructured Thin Films II*, edited by Geoffrey B. Smith, Akhlesh Lakhtakia, Cheng-Chung Lee, Proceedings of SPIE Vol. 7404 (SPIE, Bellingham, WA, 2009) Article CID Number.

ISSN 0277-786X
ISBN 9780819476944

Published by
SPIE
P.O. Box 10, Bellingham, Washington 98227-0010 USA
Telephone +1 360 676 3290 (Pacific Time) · Fax +1 360 647 1445
SPIE.org

Printed in the United States of America.

Publication of record for individual papers is online in the SPIE Digital Library.

SPIE Digital Library
SPIEDigitalLibrary.org

Paper Numbering: Proceedings of SPIE follow an e-First publication model, with papers published first online and then in print and on CD-ROM. Papers are published as they are submitted and meet publication criteria. A unique, consistent, permanent citation identifier (CID) number is assigned to each article at the time of the first publication. Utilization of CIDs allows articles to be fully citable as soon they are published online, and connects the same identifier to all online, print, and electronic versions of the publication. SPIE uses a six-digit CID article numbering system in which:

- The first four digits correspond to the SPIE volume number.
- The last two digits indicate publication order within the volume using a Base 36 numbering system employing both numerals and letters. These two-number sets start with 00, 01, 02, 03, 04, 05, 06, 07, 08, 09, 0A, 0B … 0Z, followed by 10-1Z, 20-2Z, etc.

The CID number appears on each page of the manuscript. The complete citation is used on the first page, and an abbreviated version on subsequent pages. Numbers in the index correspond to the last two digits of the six-digit CID number.

Contents

Conference Committee

Symposium Chairs

David L. Andrews, University of East Anglia Norwich (United Kingdom)
James G. Grote, Air Force Research Laboratory (United States)

Conference Chairs

Geoffrey B. Smith, University of Technology, Sydney (Australia)
Akhlesh Lakhtakia, The Pennsylvania State University (United States)
Cheng-Chung Lee, National Central University (Taiwan)

Program Committee

Ibrahim S. Abdulhalim II, Ben-Gurion University of the Negev (Israel)
Richard J. Blaikie, University of Canterbury (New Zealand)
Michael J. Brett, University of Alberta (Canada)
Didier Felbacq, Université Montpellier II (France)
Dentcho A. Genov, Louisiana Tech University (United States)
Tom G. Mackay, University of Edinburgh (United Kingdom)
Raúl J. Martín-Palma, Universidad Autónoma de Madrid (Spain)
Philip J. Moriarty, The University of Nottingham (United Kingdom)
Albert Polman, FOM Institute for Atomic and Molecular Physics (Netherlands)
Katyayani Seal, Oak Ridge National Laboratory (United States)
Motofumi Suzuki, Kyoto University (Japan)
Cuong Ton-That, University of Technology, Sydney (Australia)
Jian Xu, The Pennsylvania State University (United States)

Session Chairs

1 Optical Properties/Metamaterials
Tom G. Mackay, University of Edinburgh (United Kingdom)

2 Nanostructure and EM
Timothy J. Davis, Commonwealth Scientific and Industrial Research Organisation (Australia)

3 Semiconductors and Oxides
Cheng-Chung Lee, National Central University (Taiwan)

4 Polymers and Nanocomposites
Gunnar Westin, Uppsala University (Sweden)

Invited Paper

Comparisons of enhanced absorption in closely-coupled grating-mirror and random particle-mirror systems

Matthew D. Arnold*[a], Geoffrey B. Smith[a]
[a]Institute for Nanoscale Technology, Department of Physics and Advanced Materials, University of Technology Sydney, PO Box 123, NSW 2007, Australia

ABSTRACT

The grating-mirror geometry is a particularly rich plasmonic system due to the coupling of localized and global modes, and it is applicable to negative index materials, plasmonic imaging, and spectral filters. Recently absorption in sub-percolative films was found to be greatly enhanced by the addition of a mirror - a situation that is also reasonably modeled by a grating-mirror geometry. A great deal of attention has been focused on the coupling of barely-sub-wavelength periodic grating modes to surface plasmon polaritons that exhibit sharp spectral features. In contrast, island films have only quasi-periodicity at a few tens of nanometers, and produce broader spectral features, suggesting the influence of localized surface plasmons. In this work we examine how absorption is affected by variations in geometry of grating-mirror systems, to identify basic physics for future investigations of particle-mirror systems.

Keywords: Metal-island films, total absorption, surface plasmons

1. INTRODUCTION

Evaporation of metal onto dielectric substrates results in beading of the metal into islands prior to percolation, which can be seen in Figure 1, and the resulting metal islands exhibit interesting absorptive modes that become quite significant near percolation. Recently it has been noted when sub-percolative silver-island films are grown some distance above a relatively flat silver film, very strong absorption is observed over a wide spectral range in the near-infrared, which differs significantly from the islands alone. Figure 1 shows that absorption strengthens and red-shifts as percolation is approached. In order to fully understand this phenomenon, we seek appropriate theoretical models. One such model is the grating-mirror geometry, where a periodic grating is suspended above a metal mirror, and in particular we will focus on gratings which are invariant in one direction (as shown in Figure 2) in order to simplify calculation and analysis. Whilst this geometry is easy to analyze, it does have limitations compared to the actual system that we are trying to model. Metal-island films have only quasi-periodicity, and they are inherently structured in both dimensions. However, the grating-mirror model is a useful first step to understanding this complex geometry.

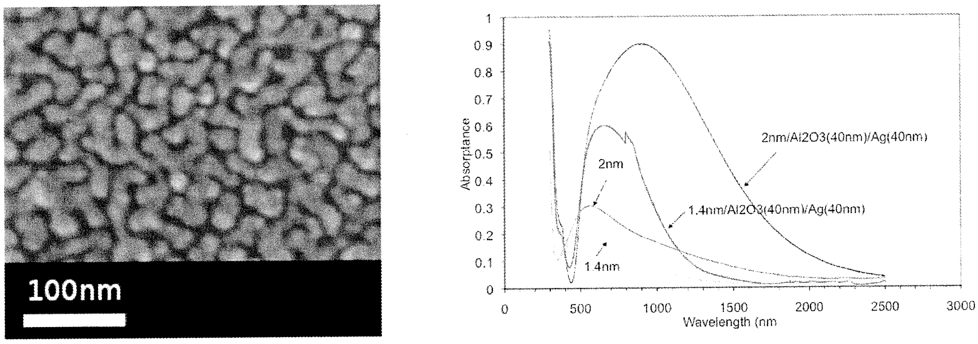

Figure 1. Electron micrograph showing sub-percolative metal island films (left) and evolution of absorptance (right).

*matthew.arnold-1@uts.edu.au; phone 61 2 9514-9715; fax 61 2 9514-2219; www.uts.edu.au

Nanostructured Thin Films II, edited by Geoffrey B. Smith, Akhlesh Lakhtakia, Cheng-Chung Lee,
Proc. of SPIE Vol. 7404, 740407 · © 2009 SPIE · CCC code: 0277-786X/09/$18 · doi: 10.1117/12.828125

An important part of the grating-mirror model is the grating itself, since it is this that controls the coupling of radiation via resonant scattering into different modes. Scattering of rays into a well-defined set of angles is the most basic property of grating modes, but it well known that there is much exciting physics beyond this. Wood noted anomalous absorption of gratings in situations corresponding to a mode traveling parallel to the surface. Ebbesen[1] observed that transmission of periodic arrays of sub-wavelength holes is enhanced compared to effective medium models based on geometric arguments. Despite the absence of multiple propagating orders, the grating can be partially reconstructed in the near-field, with obvious applications to photolithography. All of these are the result of coupling of surface states of some sort, whether evanescent waves, surface plasmon polaritons (SPP)[2], or localized surface plasmons (LSP)[3], and the discussion of the relative contribution in various situations is on-going and extensive. While SPPs are obviously important in gratings, LSPs apply to a wider range of structures, and result in interesting phenomena such as the strong absorption of nanoparticles[3], of which metal-island films are a particular type. Three-dimensional arrays of electrical and magnetic resonators can be constructed from non-magnetic metals producing negatively refracting materials, which is an active research field in its own right. Pendry[4] predicted that impedance matched negatively refracting materials can reconstruct the evanescent fields of a grating creating a super-resolving lens, and that in fact a flat film of metal is sufficient under the right conditions.

It is important to understand that the metal "lens" proposed by Pendry is also a reflector, and affects the imaging process quite strongly[5]. In addition, it can be used as a type of super-mirror to improve the quality of near-field images by increasing the depth-of-field[6]. The phase of the reflection is an important consideration, and notably the phase at the plasmonic operating point is a quarter-cycle different from that at longer wavelengths where the metal is a "good" reflector[7]. The unusual reflection phase at the edge of the SPP band is responsible for the suppression of resonant modes of the gratings. The grating-mirror geometry has been considered in other contexts, and for example it has been deduced that some modes of this system exhibit negative effective permeability[8]. Resonant transmission is observed with sharp spectral features[9-15], some of which are consistent with cavity modes, SPP modes of the mirror, and mixed LSP modes. Along with resonant transmission, resonant absorption is possible[9], which would be of great interest for use in capture of solar energy[16].

Grating mirror systems investigated so far have revealed some interesting physics, including relatively broad angular response for arbitrary polarization[17], characteristic shifting with geometry, and the importance of an appropriate thickness of grating[18]. However, these have mostly focused on barely sub-wavelength periods that are much larger than metal-islands, and only varied one parameter at a time. In this article we will investigate geometries more appropriate to metal-island films, and simultaneously vary all geometric parameters so that we can fully appreciate the global system behavior.

2. METHODS

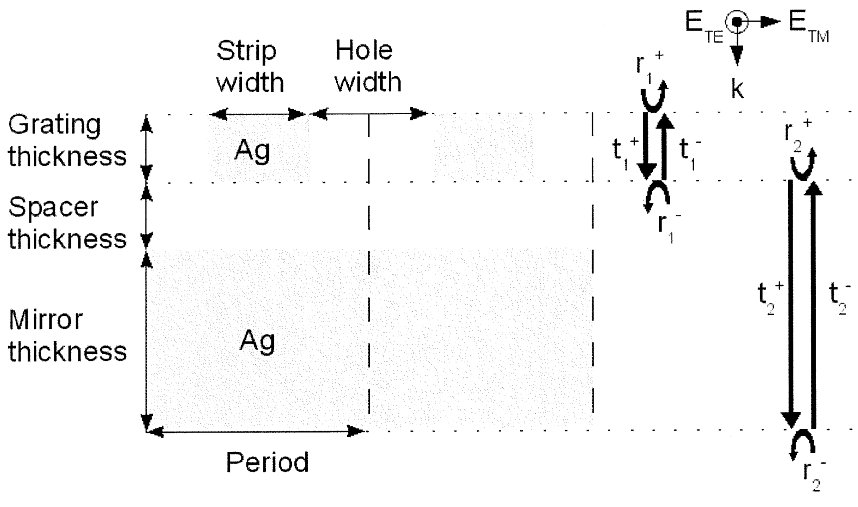

Figure 2. cross-section view of model geometry together with notation for remittance calculations and source polarization.

We used rigorous coupled wave analysis (RCWA) to efficiently calculated remittances for a large parameter sweep. RCWA couples structural eigenmodes in spatial frequency-space to plane-wave excitations in uniform layers, which is the reason for its efficiency. It is known that there may be numerical difficulties under some circumstances, but our initial tests indicate that the implementation used produced stable results, and some basic test comparisons to commercial finite element solvers (as used in) were satisfactory. In particular, we used the freely available CAMFR package to calculate the scattering matrices of the gratings[19-20], and separately calculated the remittances of the spacer/mirrors analytically[21], with careful combination of the results.

Briefly, we may denote the complex scattering matrices of the grating as r_1 and t_1, and the diagonal scattering matrices of the mirror , including spacer, as r_2 and t_2. Strictly this should include different senses of propagation, that is either forward (+) or reverse (-) directions, as shown in Figure 2. The grating matrices are calculated by CAMFR for $Ee^{j\omega t}$ and $He^{j\omega t}$ coefficients, where E and H are the electric and magnetic fields for TE and TM respectively. On the other hand we calculated the mirror matrices using the method outlined in Hodgkinson & Wu[21], which assumes $E_t e^{-i\omega t}$ coefficients, where E_t is the projection of the electric field tangential to the planar interfaces. In this case it was also necessary to normalize the internal calculations for the "phase" factor to prevent overflow of the reflected evanescent waves. In combining the two results it is essential to correctly match the various conventions, especially when calculating the energy fluxes, so we verified that our resulting fluxes matched full CAMFR calculations. The scattering matrices of the system, with multiplication transforming from incoming to outgoing waves, were given by

$$r^+ = r_1^+ + t_1^- r_2^+ \left[I - r_1^- r_2^+ \right]^{-1} t_1^+ , \quad (1)$$

$$t^+ = t_2^+ \left[I - r_1^- r_2^+ \right]^{-1} t_1^+ , \quad (2)$$

and then the fluxes were calculated using the only propagating mode resulting from normal incidence illumination – matrix index (00) - and all vacuum media. In particular the absorptance was given by

$$A = 1 - |r_{(00)}|^2 - |t_{(00)}|^2 . \quad (3)$$

This strategy makes scanning the spacer distance particularly economical – calculating the combined results for all spacer distances took an additional amount of time about the same as the grating on its own. We used N=50 modes either side of zeroth order, which is an oversampling on the order of five times compared to the minimum features used. There was no obvious difference observed between N=20 & N=50. The calculation time grows roughly as $O(N^3)$, so we opted not to extend the number of orders at this stage. A summary of the parameters used in the simulation is shown in Table 1, and we discuss further details below.

Table 1. Summary of parameter values investigated.

Parameter	Value
Incidence Angle	0° (normal)
Incidence Polarization	Linear orthogonal (TE, TM)
Incidence Wavelengths	$0.3 < \lambda < 3.0\mu m$
Metal permittivity (grating, mirror)	Ag as per CRC[22]
Media permittivity (cover, spacer, substrate)	1
Strip width	0.01, 0.02, 0.05μm
Hole width	0.01, 0.02, 0.05μm
Grating thickness	0.01, 0.02, 0.05μm
Spacer thickness	$0.0005 < d < 0.5\mu m$
Mirror thickness	1μm

Normal incidence was assumed, and we calculated both polarizations, which we refer to as TE (electric field along the invariant direction), and TM (electric field along the grating vector). We varied the each of the grating sizes (grating thickness, metal strip width, and dielectric hole width) through 5, 10, 20, 50nm, which is larger than the range of sizes expected in metal-islands. It was important not to vary the strip:hole ratio too much to avoid over-stretching the accuracy of the RCWA calculation given the number of orders used.

The spacer distance was varied from 0.5nm to 500nm using 281 log steps. This covers all possible modes adequately, although it is worth noting that at the minimum spacing field non-locality of the dielectric function is likely to be observed, which we chose not to account for in order to keep the interpretation simple. The mirror was taken to be 1000nm thick, to avoid complicating the analysis by splitting of the mirror SPP, and transmission was always less than 10^{-5}.

Bulk silver was assumed for both the gratings and the mirror. We used permittivity values interpolated from some tabulated data in the literature[22]. There is considerable variation among authors, but since this is a model system the precise value is of little consequence. Ultimately experimental verification is necessary to ensure accurate results. We used a log-wavelength scale with 91 steps from 300 to 3000nm. The choice of endpoints is somewhat arbitrary, being similar to the range that we can access experimentally, but it covers all modes satisfactorily. Conversely the spacing is quite deliberate – it is the minimum to reasonably resolve local modes of silver resonators, which are expected to have quality factors less than 40, and indeed it is observed to be adequate. The metal parts are assumed to be embedded in a vacuum – this was an arbitrary choice justifiable because we are most interested in basic physics. Embedding media will change the numerical results but likely not the overall conclusion. Once the nature of the modes is understood it should be relatively straightforward to predict the results of changing the media.

3. RESULTS

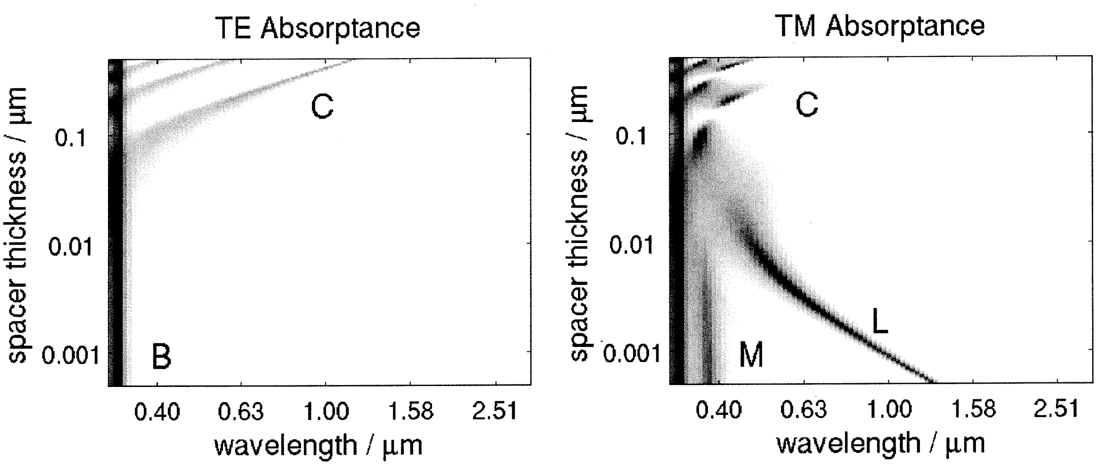

Figure 3. example of system modes for a grating of thickness 20nm with strip widths 50nm and hole widths 50nm. Dark color indicates strong absorptance. Various modes can be identified: B=bulk, C=cavity, M=grating, L=gap.

We begin with an example of a particular grating, to show the general form of modes in the wavelength-spacer plane. In Figure 3 we can identify the various modes that we will later discuss in depth. Both polarizations show strong absorption near the absorption band of bulk silver, which is also clearly evident in the mirror itself. We exclude this region from later analyses, and will not consider it further except to say that it is slightly modulated by spacer distance, and it would be interesting to consider systems where the mirror is composed of a different metal than the grating. In the TE polarization there is only one type of geometrical mode present, and it is clear from the nearly linear wavelength-spacer dependence that these are cavity modes related to the spacer. The TM polarization has three types of modes that are complicated by mixing. As with TE, cavity modes are evident, but these are broken up near a particular wavelength. Small spacer distances show two types of modes – one at a fixed wavelength that is associated with the isolated grating mode, and one with approximately inverse wavelength-spacing scaling that we assert is a plasmonic gap mode.

3.1 TE cavity modes

As seen in Figure 3, the wavelength-spacer dependence of these modes is approximately, but not exactly, linear, due to phase effects at the interfaces. Some of this can be attributed to the phase of the mirror changing phase with wavelength, however some is due to the grating itself since there are minor variations in position with different gratings. We have not considered the mode position in detail, but we have investigated the strength of the system modes in relation to those of the grating itself. Note particularly that the system modes are always much stronger than that of the isolated grating. In the TE polarization, the grating mode lies near the bulk absorption band, and so in the remaining wavelength range where the cavity modes are most evident, the grating is typically highly reflective and not very transmissive. Figure 4 shows a clear correlation between the highest reflective grating modes and strongest cavity modes. We investigated the effect of many system parameters, both individually and in combination, but only some of these were found to significantly affect the grating and hence the cavity modes. Firstly to achieve strong modes the grating should be thick enough – 10nm thickness does not seem to allow maximum absorption, whereas 20 and 50nm do. Second the hole should not be wider than the strip (see Figure 6 for example) – and as we shall see this condition is observed several times throughout the analysis.

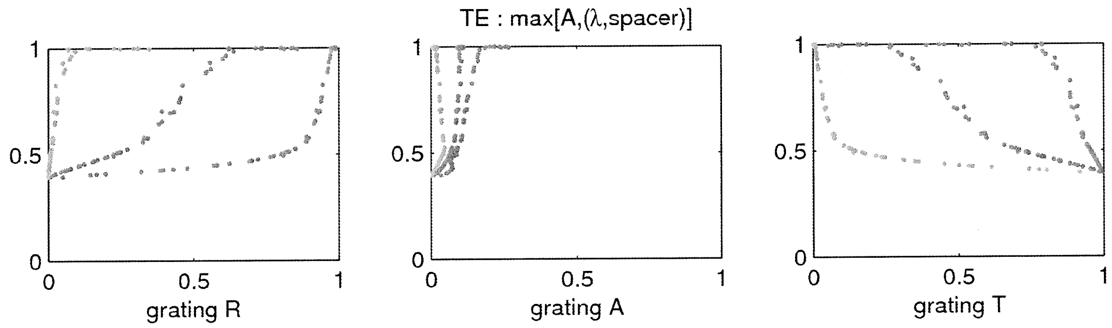

Figure 4. correlation of TE mode strength for isolated gratings compared to those of the corresponding system. Each dot represents the system mode strength maximized over all wavelengths and spacer thicknesses, as a function of the minimum (red), mean (blue), and maximum (green) remittances of the grating.

3.2 TM grating mode

We have examined the correlation between grating characteristics and the maximum strength of system TM modes across all spacings and wavelengths, since it can be difficult to isolate the modes. Once again, the strength of the system modes is correlated to those of the isolated grating, even if the system modes occur at different wavelengths to those of the grating. The maximum system mode is always more absorbing than the isolated grating mode. In particular, Figure 5 shows that strong grating modes with significant absorption peaks and suppressed transmission result in the strongest system modes. We investigated the effect of many system parameters, both individually and in combination, but only two were strongly correlated to grating absorption. Figure 6 shows that to achieve strong grating absorption under TM illumination the holes should not be wider than the strips, although thicker gratings are less sensitive to this effect. We have also considered the position of the isolated grating mode, and the strongest correlation was found with the ratio of strip width to thickness, with flatter strips leading to longer wavelengths (Figure 6).

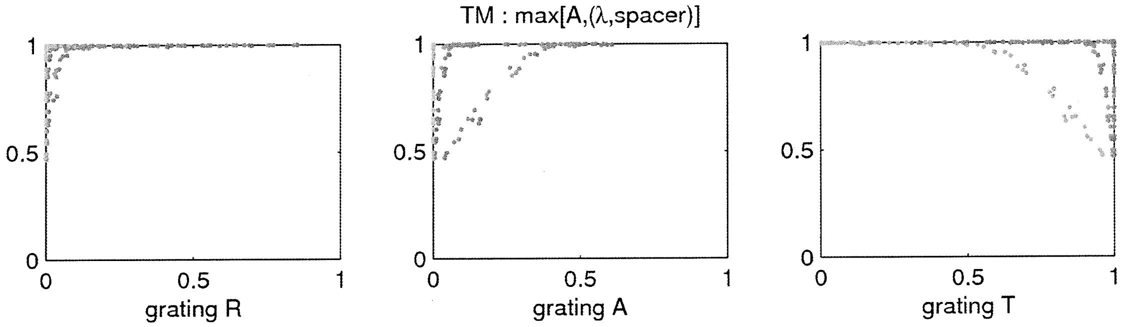

Figure 5. correlation of TM mode strength for isolated gratings compared to those of the corresponding system. Each dot represents the system mode strength maximized over all modes, wavelengths and spacer thicknesses, as a function of the minimum (red), mean (blue), and maximum (green) remittances of the grating.

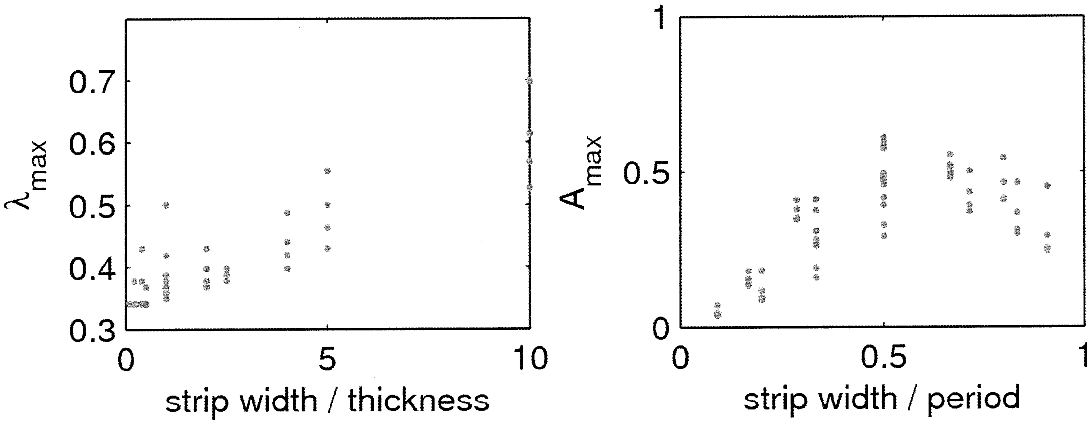

Figure 6. Main scaling of TM isolated grating absorption mode for all gratings, showing (a) the mode wavelength as a function of the ratio of strip width to thickness, and (b) the absorption of the mode as a function of the ratio of strip width to period.

3.3 TM gap mode

The gap mode is perhaps the most interesting because it requires close interaction between the grating and mirror. For each grating, we located the wavelength of strongest absorption when the spacer thickness was d=0.5nm as in the blue dot in Figure 7. The resulting wavelength and absorption was then compared to the grating parameters in Figure 8. Yet again, we find that strong modes require that the strip is at least as wide as the hole. Conventionally gap modes are plasmonic modes of the gap of a metal-dielectric-metal system, and it might be expected that the grating couples into these modes at a particular permittivity via its periodic structure. However, we find that scaling of the gap mode permittivity is best explained by the strip width compared to the spacer thickness, which is perhaps indicative of LSP-type character. To demonstrate this scaling, in Figure 7 we show a gap mode overlaid on the earlier example, using

$$w/d \sim -1.1\varepsilon\ , \tag{4}$$

where w is the strip width d is the gap thickness, and ε is the real part of the permittivity at the corresponding wavelength. In Figure 8, this same model is compared to numerically determined mode positions. The figures indicate that this is a reasonable model, at least for small gaps sizes or narrow strips.

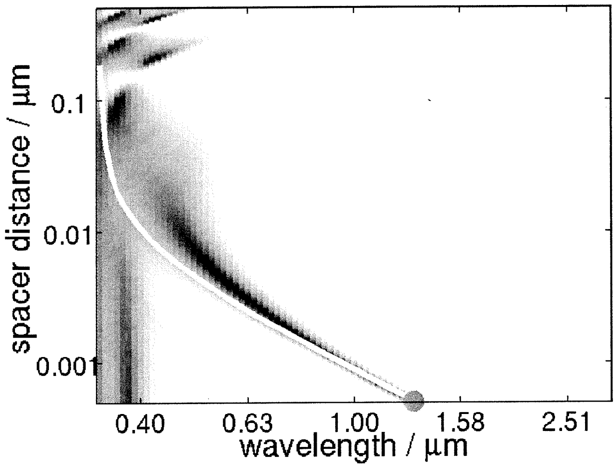

Figure 7. example of TM absorption modes (dark colors) overlaid with the gap dispersion (cyan curve) and the mode wavelength at the minimum spacer thickness (blue dot). The numerically determined wavelength forms one measurement in the figure below, and also the same gap dispersion model given by (4) is used.

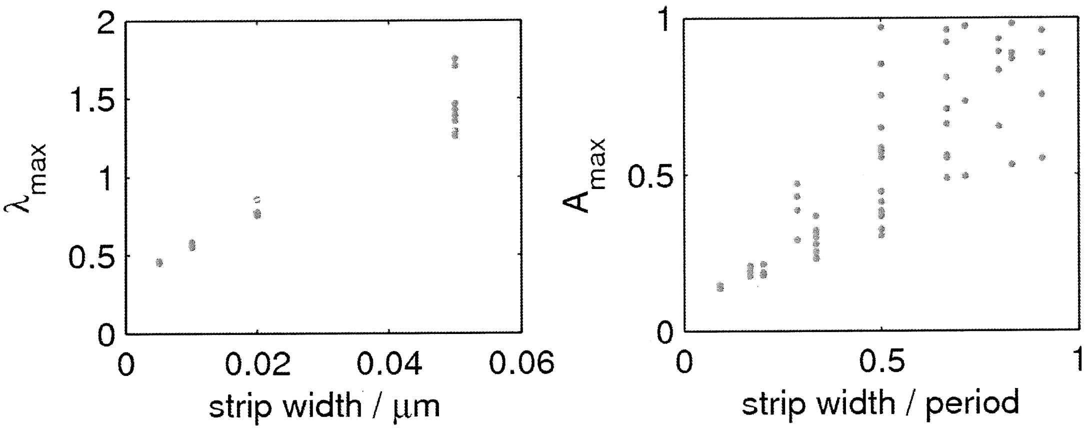

Figure 8. Main scaling of TM gap absorption mode for all gratings, showing (a) the mode wavelength as a function of the strip width, and (b) the absorption of the mode as a function of the ratio of strip width to period.

4. CONCLUSION

In conclusion we have examined the modes of silver grating-mirror systems with small feature sizes, with a reasonably comprehensive parameter sweep, using an implementation of RCWA. We found several types of modes, which in general are strongly correlated with those of the isolated grating, but considerably more absorbing. The TM case is particularly interesting, with mixing of cavity, grating, and gap modes. To achieve strongly absorbing system modes, the grating should be designed with holes narrower than the strips, and the grating thickness should be greater than 10nm. The positioning of the modes in wavelength is generally correlated to the strip width, with wider modes leading to longer wavelengths. Specifically the grating mode itself depends on the ratio of strip width to grating thickness, whereas the gap mode depends on the ratio of strip width to spacer thickness. The modes undergo significant mixing, and some broadening, especially around the spacer thicknesses that are experimentally accessible. In the future we plan to examine the mixing of these states, and generalize the results to random systems like the island-mirror systems that inspired this work. It would be interesting to examine the relative absorption in different metals and spacer materials.

REFERENCES

1. Ebbesen, T.W., Lezec, H.J., Ghaemi, H.F., Thio, T. and Wolff, P.A., "Extraordinary optical transmission through sub-wavelength hole arrays", Nature 391, 667-669 (1998).
2. Raether, H. "Surface Plasmons on Smooth and Rough Surfaces and on Gratings", Springer Tracts in Modern Physics, Springer, (1988).
3. Bohren C. F., and Huffman, D. R., "Absorption and scattering of light by small particles", Wiley, Weinheim, (2004).
4. Pendry, J.B., "Negative refraction makes a perfect lens", Phys. Rev. Lett. 85, 3966-3969 (2000)
5. Moore, C. P., Blaikie, R. J. and Arnold, M. D., "An improved transfer-matrix model for optical superlenses", Optics Express 17, 14265 (2009)
6. Arnold, M.D., and Blaikie, R.J., "Using surface-plasmon effects to improve process latitude in near-field optical lithography", Proc. ICONN 1, 548-551 (2006).
7. Arnold, M.D., and Blaikie, R.J., "Subwavelength optical imaging of evanescent fields using reflections from plasmonic slabs", Optics Express 15, 11542-11552 (2007).
8. Lin, L., and Blaikie, R.J., "Negative permeability using planar-patterned metallic multilayer", J Opt A 9, S385-S388 (2007)
9. L. Lin, R.J. Reeves, and R.J. Blaikie, "Surface-plasmon-enhanced light transmission through planar metallic films", Phys. Rev. B, 74, 155407:1-6, (2006)
10. Christ, A., Zentgraf, T., Tikhodeev, S. G., Gippius, N. A., Kuhl, J. and Giessen, H., "Controlling the interaction between localized and delocalized surface plasmon modes: Experiment and numerical calculations" Phys. Rev. B 74, 155435 (2006)
11. Jung, J. and Søndergaard, T., "Gap plasmon-polariton nanoresonators: Scattering enhancement and launching of surface plasmon polaritons", Phys. Rev. B 79, 035401 (2009)
12. Ghoshal, A., Webb-Wood, Mazuira, G. C., and Kik, P. G. "Coherent far-field excitation of surface plasmons using resonantly tuned metal nanoparticle arrays", Proc. SPIE 5927, 14 (2005)
13. Ghoshal, A., and Kik, P. G., "Optimization of Surface Plasmon Excitation Using Resonant Nanoparticle Arrays above a Silver Film", Proc. SPIE 6641, 19 (2007)
14. Ghoshal, A., and Kik, P. G., "Theory and simulation of surface plasmon excitation using resonant metal nanoparticle arrays", J. Appl. Phys. 103, 113111 (2008)
15. Ghoshal, A., Divliansky, I., and Kik, P. G., "Experimental observation of mode-selective anticrossing in surface-plasmon-coupled metal nanoparticle arrays" Appl. Phys. Lett 94, 171108 (2009)
16. Nakayama, K., Tanabe, K. and Atwater, H. A., "Plasmonic nanoparticle enhanced light absorption in GaAs solar cells", Appl. Phys. Lett. 93, 121904, (2008)
17. Wu, C., Avitzour, Y., and Shvets, G., "Ultra-thin wide-angle perfect absorber for infrared frequencies", SPIE 7029, 70290W (2008)
18. Hu, C., Zhao, Z., Chen, X., and Luo, X., "Realizing near-perfect absorption at visible frequencies", Optics Express 17, 11039-11044 (2009)
19. Bienstman, P., "Rigorous and efficient modelling of wavelength scale photonic components", PhD thesis, University of Gent (2001).
20. http://camfr.sourceforge.net
21. Hodgkinson, I.J., and Wu, Q.H., "Birefringent thin films and polarizing elements", World Scientific, (1997).
22. Weaver, J. H. and Frederikse, H. P. R., "Optical properties of selected elements", CRC Handbook 82 ed., CRC Press, Boca Raton, (2001).